

Accepted Manuscript

The time structure of neutron emission during atmospheric discharge

A.V. Gurevich, V.P. Antonova, A.P. Chubenko, A.N. Karashtin, O.N. Kryakunova, V.Yu. Lutsenko, G.G. Mitko, V.V. Piskal, M.O. Ptitsyn, V.A. Ryabov, A.L. Shepetov, Yu.V. Shlyugaev, W.M. Thu, L.I. Vildanova, K.P. Zybin



PII: S0169-8095(15)00179-9
DOI: doi: [10.1016/j.atmosres.2015.06.004](https://doi.org/10.1016/j.atmosres.2015.06.004)
Reference: ATMOS 3426

To appear in: *Atmospheric Research*

Received date: 5 February 2015
Revised date: 4 May 2015
Accepted date: 4 June 2015

Please cite this article as: Gurevich, A.V., Antonova, V.P., Chubenko, A.P., Karashtin, A.N., Kryakunova, O.N., Lutsenko, V.Yu., Mitko, G.G., Piskal, V.V., Ptitsyn, M.O., Ryabov, V.A., Shepetov, A.L., Shlyugaev, Yu.V., Thu, W.M., Vildanova, L.I., Zybin, K.P., The time structure of neutron emission during atmospheric discharge, *Atmospheric Research* (2015), doi: [10.1016/j.atmosres.2015.06.004](https://doi.org/10.1016/j.atmosres.2015.06.004)

This is a PDF file of an unedited manuscript that has been accepted for publication. As a service to our customers we are providing this early version of the manuscript. The manuscript will undergo copyediting, typesetting, and review of the resulting proof before it is published in its final form. Please note that during the production process errors may be discovered which could affect the content, and all legal disclaimers that apply to the journal pertain.

The time structure of neutron emission during atmospheric discharge

A.V. Gurevich^a, V.P. Antonova^b, A.P. Chubenko^a, A.N. Karashtin^c,
O.N. Kryakunova^b, V.Yu. Lutsenko^b, G.G. Mitko^a, V.V. Piskal^d,
M.O. Ptitsyn^a, V.A. Ryabov^a, A.L. Shepetov^a, Yu.V. Shlyugaev^e,
W.M. Thu^f, L.I. Vildanova^d, K.P. Zybin^a

^a*P.N. Lebedev Physical Institute of RAS, Moscow, 119991, Russia*

^b*Institute of Ionosphere, National Center for Space Research and Technology, Almaty, 050020, Kazakhstan*

^c*Radiophysical Research Institute, Nizhny Novgorod, 603950, Russia*

^d*Tien-Shan Mountain Cosmic Ray Station, Almaty, 050020, Kazakhstan*

^e*Institute of Applied Physics of RAS, Nizhny Novgorod, 603950, Russia*

^f*Moscow Institute of Physics and Technology. State University, Moscow, 117303, Russia*

Abstract

The time structure of neutron count rate enhancement during thunderstorm is studied. The enhancements take place during the time of atmospheric discharge. Significant part of neutrons are emitted in short bursts (200-400 μ s). Sometimes the emission is well correlated over the space scale 1 km. Short burst width allows to suppose that neutrons are generated mainly in a dense medium (probably soil).

Keywords: thunderstorm, neutrons

PACS: 52.80.Mg, 28.20.Gd

Email address: alex@lpi.ru (A.V. Gurevich)

1 **1. Introduction**

2 Last years high-energy physics in thunderstorm atmosphere attracts a
3 great attention (Dwyer and Uman (2014)). The study of energetic particle
4 fluxes (photons, electrons, positrons, muons and neutrons) make a link be-
5 tween processes developing in small subatomic scales with quite a classical
6 large scale phenomena – an atmospheric discharge.

7 Intensification of the neutron flux during thunderstorm was discussed
8 beginning from Shaha et al. (1985). The enhancements of neutron monitor
9 (NM, 6NM64 type) count rate were identified by Dorman et al. (1985) at
10 Emilio Segre' Observatory on Mt. Hermon (2025 m a.s.l.). Later the research
11 group from Aragats Space Environmental Center (3250 m a.s.l.) has observed
12 simultaneously the neutron count rate enhancement in one-minute time series
13 of NM (18NM64 type) data and the high-energy gamma-ray emission (up to
14 50 MeV) (Chilingaryan et al. (2010)). It allowed to claim that the high-
15 energy gamma-ray flux generates neutrons in atmosphere in photo-nuclear
16 reactions with air atoms.

17 A new important step was done by Tsuchiya et al. (2012) at Yangbajing
18 Cosmic Ray Observatory (Tibet, altitude 4300 m a.s.l.). The simultaneous
19 measurements in five-minute time series of neutron count enhancements in
20 NM (28NM64 type) and of high-energy (up to 160 MeV) gamma-ray emission
21 flux during an intensive thunderstorm were fulfilled. Combining the results
22 of measurements with numerical calculations the authors have stated that
23 additional neutrons forming neutron count enhancements are born mainly
24 not in atmosphere but inside the NM. In other words it was supposed that
25 the environmental neutron enhancement does not play any essential role, and

26 the observed additional neutrons are generated by energetic gamma quanta
27 in the NM directly. Gamma quanta themselves are supposed to be generated
28 by electrons accelerated in quasi-stable thunderstorm electric field. Aragats
29 group afterwards reconsidered the previous statement and found that both
30 photo-nuclear processes in the air and in NM should be considered to explain
31 the neutron fluxes (Chilingaryan et al. (2012)).

32 Gurevich et al. (2012) have reported the results of neutron flux mea-
33 surements at Tian-Shan Cosmic Ray Station (altitude 3340 m a.s.l.) dur-
34 ing summer 2010 thunderstorms. The NM (18NM64 type) and three low-
35 energy neutron detectors were used simultaneously. For the first time the
36 intensive fluxes of low-energy neutrons generated during thunderstorms have
37 been registered. The correlation of the neutron count rate enhancements
38 in one-minute time series with simultaneously measured electric field vari-
39 ations allowed to claim that the neutron flux enhancements are connected
40 with atmospheric discharges.

41 It should be noted, that the enhancements of neutron flux were registered
42 not only in mountains but also at the low ground level (Kozlov et al. (2013))
43 and even in laboratory high-voltage atmospheric discharge (Agafonov et al.
44 (2013)).

45 The time structure of the neutron flux enhancement in high resolution
46 ($200 \mu\text{s}$) time series was studied during the summer 2013 thunderstorms
47 using the modified installation at the Tien-Shan Station. We are reporting
48 here the results of these observations. It is established that the neutrons are
49 generated during thunderstorm atmospheric discharges. Often the neutrons
50 are emitted in short bursts; the burst width is 200-400 μs . Besides, the bursts

51 with longer width (up to 3-10 ms) were observed as well. Neutron count
52 bursts are observed simultaneously by six independent detectors situated at
53 the distance about 1 km from each other; often the bursts of distant detectors
54 are well time-correlated. Mainly the observed neutrons had low energies, less
55 than 1 keV, though in a part of the bursts the energy is higher.

56 2. Instrumentation

57 Measurements were fulfilled on the installation “Thunderstorm” of Tien-
58 Shan Station (Gurevich et al. (2009)). The detectors used in summer 2013
59 investigation of thunderstorm neutron flux enhancements were located in two
60 points: the Station itself – *Station point*, and on the top of a neighboring
61 hill – *Hill point*. The Hill point is situated 160 m above the common level of
62 the Station; the distance between Hill point and the Station point is about
63 1 km. At the Station point we used the neutron monitor (NM) as well as
64 three low-energy ^3He neutron detectors. Two ^3He detectors were used at the
65 Hill point.

66 The Tien-Shan neutron monitor 18NM64 is sensitive mainly to the high-
67 energy hadronic flux of the cosmic ray origin (above some hundreds of MeV)
68 but is capable also to register the neutrons having energies ~ 1 MeV and
69 below with a small, 0.05-1%, probability (Gurevich et al. (2012); Chubenko
70 et al. (2003)).

71 The low-energy neutron detectors are the 1.2×0.84 m² boxes of 2 mm
72 thick aluminum each containing six 1 m long, 3 cm in diameter proportional
73 ^3He neutron counters. The pressure in the counter tube is 2 atm. These
74 counters are not surrounded by any moderator material, and thus they are

75 mostly sensitive to the low energy range ($\lesssim 1$ keV) neutrons. The placement
76 of three ^3He detectors situated at the Station point (*external*, *internal* and
77 *underfloor*) is shown in Fig. 1.

Figure 1: Placement of ^3He detectors and NM at the Station point. Ex, In and U – the external, the internal and the underfloor detectors correspondingly. A, B, C – three standard 6-counter units of the NM64 type supermonitor. An external detector is placed outdoors inside a plywood housing at the distance 15 m from other detectors. The internal detector is placed in the same room with the NM. The underfloor detector is placed under the wooden (4 cm) floor of the same room and is additionally shielded from the top by a 9 cm thick layer of rubber.

78 Two neutron detectors were installed at the Hill point. The *Hill-free*
79 detector is of the same type as those at the Station point. The *Hill-shielded*
80 detector is surrounded with moderator polyethylene tubes of 0.5 cm wall
81 thickness increasing the detector efficiency. Efficiencies of detectors situated
82 at the Station and Hill points are presented in Fig. 2.

Figure 2: Efficiencies of neutron detectors calculated with the use of GEANT4 toolkit (GEANT4 collaboration (2003)). ^3He counters: 1 – without moderator (external, internal and Hill-free detectors), 2 – with polyethylene moderator (Hill-shielded detector); 3 – underfloor detector; while evaluating it's efficiency the placement (4 cm wooden floor and the 9 cm ribbon layer above the detector) was taken into account. 4 – the neutron monitor.

83 Neutron counting rates are measured as follows. After an amplification
84 and shaping, the electric signals from each neutron counter separately are

85 connected to the multichannel pulse intensity measurement system which
86 counts the number of pulses in 10000 succeeding $200 \mu\text{s}$ long time intervals.
87 Each moment of time, this system keeps in its internal memory the temporal
88 history of the counting rate on its inputs for the last 2 s, and can write it
89 down with arrival of a special control signal — the trigger. In these records
90 the arrival moment of trigger signal coincides always with the median time
91 interval so both the pre-history of signal intensity during 1 s before the trigger
92 and its behavior in succeeding second are available with resolution of $200 \mu\text{s}$
93 in each registered event.

94 The NM registration system was supplied by an additional fast registra-
95 tion system (besides the one described above) which had a temporal resolu-
96 tion of $72 \mu\text{s}$ in a limited time space of $4000 \mu\text{s}$, and was synchronized by the
97 trigger. In favorable cases when a single peak of neutron intensity falls on
98 the first four milliseconds after the trigger the fast registration system permit
99 to resolve the temporal development of neutron signal more distinctly.

100 Simultaneously, the signals from all neutron detectors are connected to
101 another set of digital counters which continuously measure the number of
102 pulses with a raw time resolution of 10 s, without binding to any external
103 trigger. In this monitoring mode we also have used two field-mill type de-
104 tectors to measure the electric field and two NaI scintillation detectors to
105 register the gamma-ray flux. One electric field detector and one NaI detector
106 were placed at the Station point, another pair of these detectors – at the Hill
107 point.

108 The trigger signal is generated with a local electric field derivative de-
109 tector (capacitor). This is a 0.25 m^2 capacitor sensor installed outdoors in

110 NM vicinity with one of its plates being grounded. The short ($\leq 100 \mu\text{s}$)
111 electric pulses induced on the other plate of this capacitor in the moment of
112 a fast change in local electric field are connected to a threshold discriminator
113 scheme which generates trigger pulse if the signal on its input exceeds a pre-
114 defined value. After its shaping the trigger is transmitted over the shielded
115 cable simultaneously both to detector system at the Station and Hill points
116 through the powerful amplifier which is stable against the influence of strong
117 electromagnetic interferences from lightning.

118 In the trigger mode atmospheric discharges were additionally registered
119 by a radio installation working in the frequency range 0.1 to 30 MHz (Gure-
120 vich et al. (2003)).

121 A special attention was paid to reliability of signals registration in thun-
122 derstorm conditions. All the detectors were grounded and electromagnet-
123 ically shielded. The absence of electromagnetic interference on the regis-
124 tration system was controlled by using a “dummy” information channels –
125 additional ^3He counters placed inside the detector boxes which are switched
126 to the data registration system but the high voltage in the feeding main
127 is strongly diminished to exclude the neutron registration. All the signals
128 from neutron detectors including the “dummy” ones pass through the dis-
129 criminators having the same thresholds for all channels. The threshold value
130 is arranged in such a way that it is higher than the electronic circuit noise.
131 The registration system counts pulses of the discriminator output signal. The
132 number of pulses in “dummy” channels is found to be zero both in the non-
133 thunderstorm and in the thunderstorm time. Additional isolation against
134 electromagnetic influence has been constructed at the Hill point. The ply-

135 wood cabin at the Hill point containing detectors was shielded by a grounded
136 outer aluminum upholstery, and every time with storm approach its whole
137 powering is switched to internal accumulator battery. So, the neutron flux
138 measurements at the Hill were fulfilled in the absence of the outer electro-
139 magnetic influence (Faraday cage).

140 3. Observational data

141 Thunderstorm neutron enhancement observations were fulfilled in 2013
142 on the Tien-Shan Station from 12.06 till 24.07. Twenty thunderstorms were
143 observed during 11 days. Both the monitoring of neutron flux with 10 s
144 accumulating time and the triggered 2 s long (1 s before and 1 s after the
145 trigger) registration was used.

146 The main result of the monitoring is that the neutron enhancements are
147 observed in the periods of thunderstorm activity only. It is illustrated in
148 Figs. 3-5. In Fig. 3 the 10 s monitoring data obtained during July 13 and
149 July 21, 2013 are presented. As it is clearly seen from the figure, the neutron
150 background flux at all the detectors is very stable during the whole day. It is
151 determined by low energy cosmic rays (CR). The primary CR particle having
152 the energy higher than 10^{17} eV generates a shower which lead to a neutron
153 enhancement lasting for about one millisecond. The flux of such CR particles
154 is 1 particle per km^2 per day. So, the probability of its coincidence in the
155 same time and place with the lightning discharge is very small, our detectors
156 being triggered by electric-field jumps do not register EAS events.

157 The noticeable neutron enhancements were observed within the storm
158 period when the intensive electric field variations and gamma-ray emission

159 are present. In more details the monitoring data obtained during the storms
160 are presented at Fig.4. The prominent neutron count rate enhancements are
161 seen on July, 13 during the thunderstorm which lasted for 30 min from 13:40
162 to 14:10 and on July, 21 at the beginning of the thunderstorm which lasted
163 from 6:30 till 13:00. Two enhancements are presented in Fig.5 with a time
164 scale zoomed in relative to that of Fig. 4. It is seen that the duration of
165 every separate enhancement is not longer than 10 s. This statement is right
166 for all registered neutron count rate enhancements.

Figure 3: Monitoring mode results during July 13 and 21, 2013. Detectors are marked in the panels.

Figure 4: Monitoring mode results during thunderstorms on July 13 and 21, 2013. Upper panel - electric field as measured by the field-mill detector placed at the Station point, lower panels - count rates in different neutron detectors marked in the panels.

Figure 5: Examples of neutron count rate enhancements registered in the monitoring mode on July, 13 and 21, 2013, presented with a time scale zoomed in. Panels are the same as in Fig. 4. Zero points marks the middle of a 10-s intervals containing the trigger moments presented in Figs. 6, 7.

167 Triggered registration was used to study the fine time structure of neu-
168 tron flux during thunderstorms. The overall number of triggered records

169 containing count rate enhancements was 39 through the 20 thunderstorms,
 170 it makes 20% of all triggered records. Durations of enhancements and main
 171 characteristics of neutron bursts observed during all the events are presented
 172 in Table 1. The enhancement duration is less than 100 ms in most cases.
 173 For example, the neutron signal during the discharge 13.07.2013 (13:56:02,
 174 see left panel of Fig. 6 and Fig. 7) lasted 100 ms, and during the discharge
 175 21.07.2013 (06:37:52, see right panel of Fig. 6 and Fig. 7) – 10 ms. But some
 176 neutron signals are longer. The longest one (23.07.2013, 09:55:56) lasted 550
 177 ms, the other enhancements of this long-term events lasted 460, 400, 350,
 178 350 and 230 ms.

Table 1: Neutron event characteristics. All columns except column NM (neutron monitor) and column C present data obtained by one of non-moderated ^3He detectors. The presented parameter value is the maximal registered at the Station point (S) or at the Hill point (H). Duration – time from the beginning of the first neutron burst to the end of the last one. Short and Long – numbers of neutron bursts shorter and greater than $400 \mu\text{s}$ correspondingly. N – the maximal neutron count in a $200 \mu\text{s}$ interval registered by a ^3He detector. C - coincidence number, i.e. a number of bursts registered simultaneously by all detectors and NM.

Event		Duration, ms			Short		Long		N		C
Date	Time	S	H	NM	S	H	S	H	S	H	
12:06:13	12:31:39	0.6	180	330	1	8	0	1	4	8	1
13:06:13	12:42:55	0.4	120	240	1	6	0	0	9	20	1
13:06:13	12:44:28	1	1.6	6.2	0	0	1	1	8	14	1
03:07:13	11:27:44	0.2	8	133	1	2	0	0	11	47	1
03:07:13	11:29:42	0.4	0.4	420	1	1	0	0	12	43	1
07:07:13	15:02:28	0.4	24	24	1	5	0	0	34	32	1
07:07:13	15:05:12	0	0.2	81	0	1	0	0	0	6	0
07:07:13	15:18:03	0.2	0	192	1	0	0	0	3	0	0
08:07:13	07:54:45	6	22	27	2	2	0	1	4	5	1
11:07:13	11:46:21	0	0.4	1.2	0	1	0	0	0	8	0
11:07:13	12:41:08	0.4	0.4	98	1	1	0	0	3	9	1
13:07:13	13:56:02	54	54	92	7	6	0	1	20	19	3
13:07:13	14:01:03	12	51	186	3	9	0	1	8	23	1
14:07:13	09:00:13	8	22	51	12	8	3	4	31	17	5
15:07:13	05:13:58	26	43	121	2	4	0	1	22	36	2

Continued on the next page

Table 1: (continued)

Event		Duration, ms			Short		Long		N		C
Date	Time	S	H	NM	S	H	S	H	S	H	
15:07:13	15:18:20	0.2	1.4	158	1	1	0	1	3	15	0
17:07:13	07:50:14	0.2	0.2	410	1	1	0	0	3	9	1
17:07:13	09:55:11	0.2	0.2	19	1	1	0	0	3	21	1
20:07:13	18:05:38	0	1.6	2.1	0	0	1	1	14	28	0
21:07:13	06:37:51	6	6.2	11	0	0	1	1	42	44	1
21:07:13	07:02:18	0.2	0.2	225	1	1	0	0	9	37	1
21:07:13	07:05:40	0.2	0.2	254	1	2	0	0	3	18	1
21:07:13	07:49:47	0.2	180	462	1	3	0	0	3	4	0
21:07:13	07:54:34	0.4	0.4	163	1	1	0	0	5	22	1
23:07:13	06:32:44	0.2	47	52	1	6	0	1	4	10	1
23:07:13	06:38:45	18	24	88	4	5	0	1	3	9	1
23:07:13	06:42:25	0.4	33	47	1	3	0	1	25	8	1
23:07:13	09:55:56	221	533	542	2	6	0	0	22	21	2
23:07:13	09:57:24	0.4	0.4	113	1	1	0	0	6	5	0
23:07:13	12:52:08	33	41	214	2	5	0	0	11	22	2
23:07:13	12:52:57	0	0.4	67	0	1	0	0	0	5	0
23:07:13	12:55:15	77	77	362	2	2	0	0	4	11	2
23:07:13	12:57:08	8	8	213	2	2	0	1	10	9	2
23:07:13	12:58:20	0.6	0.6	3.8	0	0	1	1	7	6	1
23:07:13	13:00:23	0	28	28	0	7	0	1	0	19	0
23:07:13	13:05:43	0	46	205	0	2	0	4	0	7	0
23:07:13	13:02:01	0.4	0.4	24	1	2	0	0	10	16	1
24:07:13	05:01:51	0.4	0.4	1	1	1.2	0	0	13	17	1
24:07:13	05:11:34	1.6	1.6	161	2	1	0	0	4	5	1

179

180 The main striking the eye characteristic of the enhancements registered
181 by ^3He detectors and often by NM is its burst time structure (Fig. 7). The
182 burst width in ^3He detector is usually about 1-2 registration time intervals
183 (200-400 μs). Occasionally the 3-4 registration intervals duration of bursts
184 is also observed. Such a time structure is observed both in the main part of
185 events and in the long-term ones.

Figure 6: Time structure of neutron count rate of the discharge 13 July 2013 (13:56:02) and of the discharge 21.07.2013 (06:37:52).

Figure 7: Fine time structures of neutron count rate of the discharge 13 July 2013 (13:56:02) and of the discharge 21.07.2013 (06:37:52). “n=” – the number of neutrons registered during 100 ms; “m=” – the mean number of neutrons expected for 100 ms from monitoring mode results.

186 In 13 records the count rate enhancements in neutron detectors start at
 187 the trigger moment. Six of these near-trigger enhancements are short (less
 188 than 2 ms), and seven are relatively long (3-6 ms, see Fig. 7 for an example).
 189 Significant and often even the main part of neutrons is generated during this
 190 initial milliseconds of atmospheric discharges. Sometimes these initial events
 191 are accompanied by a tail of solitary bursts.

192 The count rate enhancements are registered by NM in all cases. A number
 193 of long (up to 10 ms) time-correlated enhancements are observed both in NM
 194 and in Hill-shielded detector. In these cases the enhancements in non-shielded
 195 ^3He counters are not very prominent what indicate that neutrons observed
 196 both in NM and shielded detector are of middle energy ($1 < E < 1000$
 197 keV). For example, in the event 08.07.2013 (07:54:45) sum number of surplus
 198 neutron signals during the 10 ms long burst in NM is 430, in Hill-shielded
 199 detector – 177, in Hill-free detector – 12, in external detector – 5, in internal
 200 detector – 7, and in underfloor detector - 2.

201 A number of bursts (40 during all thunderstorms) are time-correlated in
 202 NM and in all ^3He detectors independently on where they are placed, at

203 the Station or at the Hill registration points. These bursts are short – 1-
204 2 registration intervals. Sometimes there are two time synchronized events
205 during the same discharge. For example on July, 15 (05:13:58) there were
206 two synchronized bursts in all detectors at 12 ms and 44 ms after the trigger
207 time.

208 The strong neutron enhancement at the moment of the electric field jump
209 is clearly seen in Fig.6-7. We emphasize, that the neutron signal enhance-
210 ments occur in the after-trigger second only. It should be added that during
211 the pre-trigger second the value of the count rate in all ^3He detectors agrees
212 with that obtained in the 10 s monitoring mode. We see that any neutron
213 count enhancements are absent here within the statistical error. On the other
214 hand, the enhancement after the trigger is quite prominent. It is illustrated
215 in the Fig. 7, where the number of neutrons registered during 100 ms of the
216 after-trigger time are presented. It is compared with the mean values ex-
217 pected for the same time interval from monitoring mode results. One can see
218 that the effect is very strong: the enhancement overcomes the mean value
219 in 50-300 times for all ^3He detectors! The strong effect is seen for NM as
220 well: here enhancement is 8-9 times. So, our observations demonstrate defi-
221 nitely that the strong neutron enhancements are deeply connected with the
222 lightning discharge, mainly with its initial part.

223 4. Discussion

224 Comparing the 2013 results with the 2010 results Gurevich et al. (2012)
225 we see that the neutron amount was somewhat larger in 2010. Note, that
226 this difference is more visible in the low-energy ^3He detectors than in NM.

227 The one minute integral amount of neutron enhancements observed by NM
228 are quite comparable: 900-1200 in 2013, and 600-2800 in 2010. Related to a
229 single NM unit the amplitude of neutron enhancement in 2010 reaches 140
230 per minute for strong thunderstorms, and is about 50 for a weak one, in 2013
231 the enhancement is about 60 ± 40 . These results are in accordance with the
232 results of Tibet and Aragatz groups: 140 per minute for a one NM unit for
233 the strong thunderstorm analyzed by Tibet group, and 60 for the Aragatz
234 group. Thus, one can state that the integral enhancement of neutrons during
235 thunderstorm in the averaged one minute NM data are analogous in all three
236 groups.

237 The detailed time structure of the neutron signal is shown in Fig.7. It is
238 seen that the neutrons are often observed in multiple short bursts as it was
239 mentioned above. Each burst as registered by ^3He detector lasts only 1-2
240 time intervals ($200-400 \mu\text{s}$).

Figure 8: Examples of the neutron signal time dependencies as registered by the NM fast registration system (circles with error bars). Every plot corresponds to a neutron signal peak registered just at the moment of trigger arrival. The smooth continuous lines represent the usual exponential distribution anticipated for the neutrons momentary born in the monitor and diffusing inside it later on (see text).

241 Note, that the simultaneous bursts in NM signal seem to be wider – about
242 1 ms (see Fig.6). The following consideration shows that it is an apparent
243 effect. It is well known that after a momentary generation of neutrons inside
244 NM by a high- energy cosmic ray hadron the neutron intensity grows up in a

245 microsecond time scale and after that falls down due to neutron diffusion in
246 NM. The fall is in accordance with exponential law $I(t) \sim 0.72\exp(-t/\tau_1) +$
247 $0.28\exp(-t/\tau_2)$ with lifetimes $\tau_1 \sim 240 \mu\text{s}$ and $\tau_2 \sim 650 \mu\text{s}$ (for the NM64
248 type supermonitor configuration) Hatton and Carmichael (1964); Antonova
249 et al. (2002). If to draw the corresponding distribution curves on the plots of
250 Fig. 8 one can see that the experimentally measured signal intensity agrees
251 with the expected exponential behavior. This is an evidence that we observe
252 neutrons and that the initial neutron signal lasts in NM the same short time
253 as in ^3He detectors.

254 The definite time delay (about 2-3 ms) between the initiation of neutron
255 emission at the Station and Hill registration points is seen in the right panel of
256 Fig.7. This time delay could be interpreted as the result of the atmospheric
257 discharge front motion between the points. This motion has the velocity
258 $(3 - 5) \cdot 10^7 \text{ cm s}^{-1}$ which is just the characteristic lightning velocity.

259 Neutrons propagating through the medium could be scattered and cap-
260 tured by nuclei. The both processes determine the mean free path time,
261 which is inverse proportional to the nucleon number density. The same re-
262 lates to the thermalization time when a new born neutron having initial
263 energy about 10 MeV loses it up to the thermal energy values in collisions.
264 The density of the soil is about thousand time larger than that in air at
265 the height of the Station. The evaluation of characteristic parameters of the
266 processes using standard formulas (see Galanin A.D. (1958)) shows that the
267 mean neutron free path time in a dense medium (soil, Si) is $50 \mu\text{s}$ and the
268 thermalization time is about $500 \mu\text{s}$, while in the air the neutron free path
269 time is about 20 ms, and thermalization time is 90 ms – hundreds times

270 larger. The neutron bursts which are propagating and thermalizing in the air
 271 should have the width not less than 50-100 ms – 2-3 orders of the magnitude
 272 higher than the observed one (200-400 μ s). In soil the thermalized neu-
 273 trons have the diffusion length about 17 cm, and the thermalization length
 274 from energies about 10 MeV up to the thermal energy is 115 cm. Thus,
 275 the observed width of the bursts (200-400 μ s) shows that the neutrons are
 276 generated in the ground or at its surface in a few meters around detector and
 277 propagate in soil or other environmental dense medium but not in the air. It
 278 should be noted, that the discussion of neutron registration results in Chilin-
 279 garyan et al. (2012), Babich et al. (2013), and Tsuchiya (2014) is based on
 280 the assumption that the neutrons are generated in the air or directly in the
 281 detectors, their generation and propagation in soil or other environmental
 282 dense medium are not considered at all.

283 An integral number of neutrons generated in one burst could be estimated
 284 for those events when the enhancement is observed simultaneously in all
 285 detectors both at the Station and the Hill points. Taking into account that
 286 the distance between the location points is $R \approx 1000$ m the number of
 287 neutrons generated in one short burst could be estimated as $N_b \sim R^2 \cdot I_b$,
 288 were I_b is the neutron fluence in the burst. As it follows from the Fig. 7
 289 about 10-20 neutrons are registered in one short burst. Taking into account
 290 that the efficiency of the low-energy neutron registration is about 10%, and
 291 that the effective area of the counter is about 0.5 m² the fluence I_b could
 292 be estimated as 10² m⁻². Thus, we obtain $N_b \approx 10^8$. The full number of
 293 neutrons in a long burst could be about 10⁹. The total neutron number
 294 generated during one discharge can reach $3 \cdot 10^9 - 10^{10}$.

295 5. Conclusions

296 Previously, the neutron enhancements in thunderstorm were studied only
297 with a long-scale time resolution (1-5 min). In this work the time structure
298 of the neutron count rate enhancement was studied more precisely with reso-
299 lution of 200 μ s. It is demonstrated that the enhancements take place during
300 the time of atmospheric discharge. Neutrons are emitted often in short bursts
301 lasting 200-400 μ s. Sometimes the emission is well correlated over the wide
302 space - up to 1 km scale. The full number of neutrons generated in a burst is
303 about 10^8 . Short burst width allows to suppose that neutrons are generated
304 mainly in a dense medium near the detectors, probably in soil.

305 It should be noted also, that the time structure of the neutron signal is
306 observed by three types of detectors: ^3He counters, polyethylene moderated
307 ^3He counter and the NM. All the detectors sometimes demonstrate the highly
308 correlated short pulses of neutrons. Sometimes correlated bursts are observed
309 around one point only – Station point or Hill point which are divided by a
310 large distance. In a number of events only detectors of a type sensitive to
311 neutrons of middle energy demonstrate an intensive neutron burst while other
312 detectors are silent. All this indicates that the neutrons of different energies
313 correlated in time and space are generated during thunderstorm discharge.

314 **Acknowledgments.** This work was supported by the RAS Programs
315 29II and 11O Φ and by RFBR grant #15-45-02636.

316 References

317 Agafonov, A.V., et al., 2013. Observation of neutron bursts produced by
318 laboratory high-voltage atmospheric discharge, PRL 111, 115003.

- 319 Antonova, V.P., et al., 2002. Anomalous time structure of extensive air
320 shower particle flows in the knee region of primary cosmic ray spectrum,
321 Journal of Physics G: Nuclear and Particle Physics 28, 251-266.
- 322 Babich, L.P., et al., 2013. Numerical analysis of 2010 high-mountain (Tien-
323 Shan) experiment on observations of thunderstorm-related low-energy neu-
324 tron emissions, JGR Space Physics 118, 7905-7912.
- 325 Chilingarian, A., et al., 2010. Ground-based observations of thunderstorm-
326 correlated fluxes of high-energy electrons, gamma rays, and neutrons, PRD
327 82, 043009.
- 328 Chilingarian, A., Bostanjyan, N., Karapetyan, T., Vanyan, L., 2012. Remarks
329 on recent results on neutron production during thunderstorms, PRD 86,
330 093017.
- 331 Chubenko, A.P., et al., 2003. Multiplicity Spectrum of NM64 Neutron Su-
332 permonitor and Hadron Energy Spectrum at Mountain Level, Proceedings
333 of the 28th Int. Cosmic Ray Conf., Tsukuba, 789-792.
- 334 Clem, J.M., Dorman, L.I., 2000. Neutron monitor response functions, Space
335 Sci. Rev. 93, 335-359.
- 336 Dwyer, J.R., Uman, M.A., 2014. The physics of lightning, Phys. Rep 534,
337 147-241.
- 338 Galanin, A.D. The theory of thermal-neutron nuclear reactors, New York:
339 Consultants Bureau, 1958.

- 340 Dorman, L.I. et al, 2003. Thunderstorms' atmospheric electric field effects
341 in the intensity of cosmic ray muons and in neutron monitor data, JGR
342 108(A5), 1181-1188.
- 343 Geant4 Collaboration, 2003. Geant4 - a simulation toolkit, Nuclear Instru-
344 ments and Methods in Physics 506, 250-303.
- 345 Gurevich, A.V., et al., 2003. Radio emission of lightning initiation, Phys.
346 Lett. A 312, 228.
- 347 Gurevich, A.V., et al., 2009. Effects of cosmic rays and runaway breakdown
348 on thunderstorm discharges, Physics-Uspekhi 52, 735.
- 349 Gurevich, A.V., et al., 2012. Strong flux of low-energy neutrons produced by
350 thunderstorms, PRL 108, 125001.
- 351 Hatton, C.J., Carmichael, H., 1964. Experimental investigation of the NM-64
352 neutron monitor, Canadian Journal of Physics 42, 2443.
- 353 Kozlov, V.I., Mullayarov, V.A., Starodubtsev, S.A., Toropov, A.A., 2013.
354 Neutron bursts associated with lightning cloud-to-ground discharges, Jour-
355 nal of Physics: Conference Series 409, 012210.
- 356 Shah, G.N., Razdan, H., Bhat, C.L., Ali, Q.M., 1985. Neutron generation in
357 lightning bolts, Nature 313, 773-775.
- 358 Tsuchiya H. et al., 2012, Observation of thundercloud-related gamma rays
359 and neutrons in Tibet, PRD 85, 092006.
- 360 Tsuchiya, H., 2014. Surrounding material effect on measurement of
361 thunderstorm-related neutrons, Astroparticle Physics 57-58, 33.

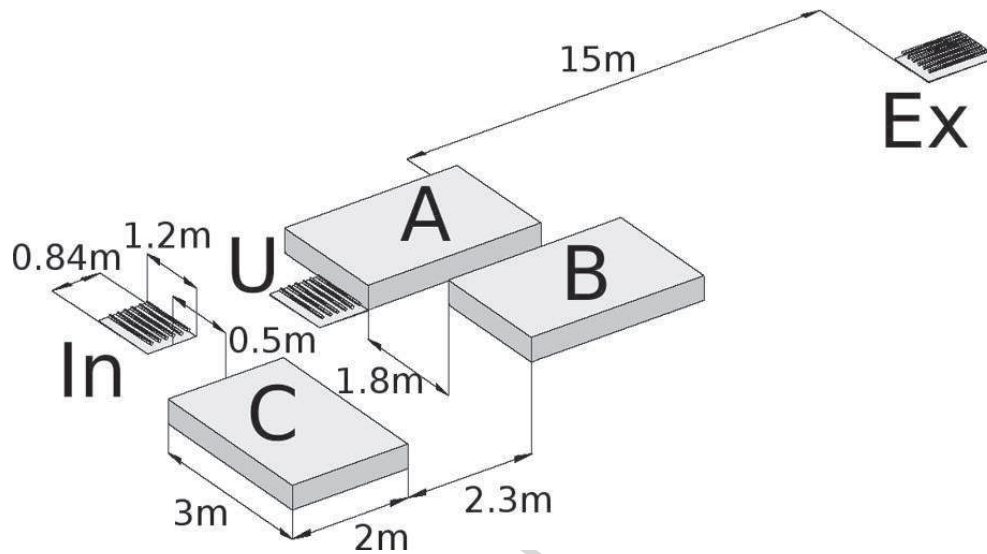


Fig. 1. Placement of ^3He detectors and NM at the Station point. Ex, In and U – the external, the internal and the underfloor detectors correspondingly. A, B, C – three standard 6-counter units of the NM64 type supermonitor. An external detector is placed outdoors inside a plywood housing at the distance 15 m from other detectors. The internal detector is placed in the same room with the NM. The underfloor detector is placed under the wooden (4 cm) floor of the same room and is additionally shielded from the top by a 9 cm thick layer of rubber.

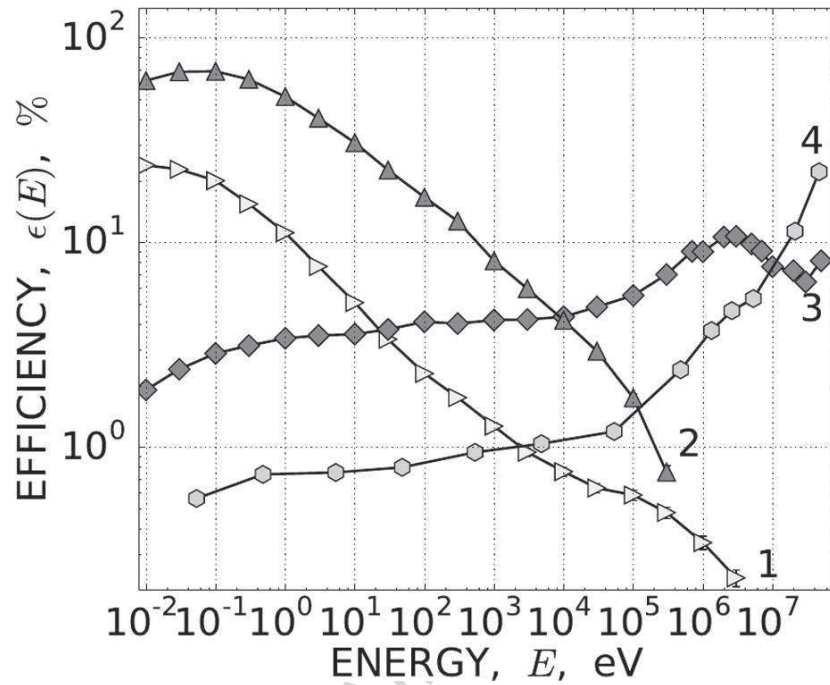


Fig. 2. Efficiencies of neutron detectors calculated with the use of GEANT4 toolkit (GEANT4 collaboration (2003)). ^3He counters: 1 – without moderator (external, internal and Hill-free detectors), 2 – with polyethylene moderator (Hill-shielded detector); 3 – underfloor detector; while evaluating it's efficiency the placement (4 cm wooden floor and the 9 cm ribbon layer above the detector) was taken into account. 4 – the neutron monitor.

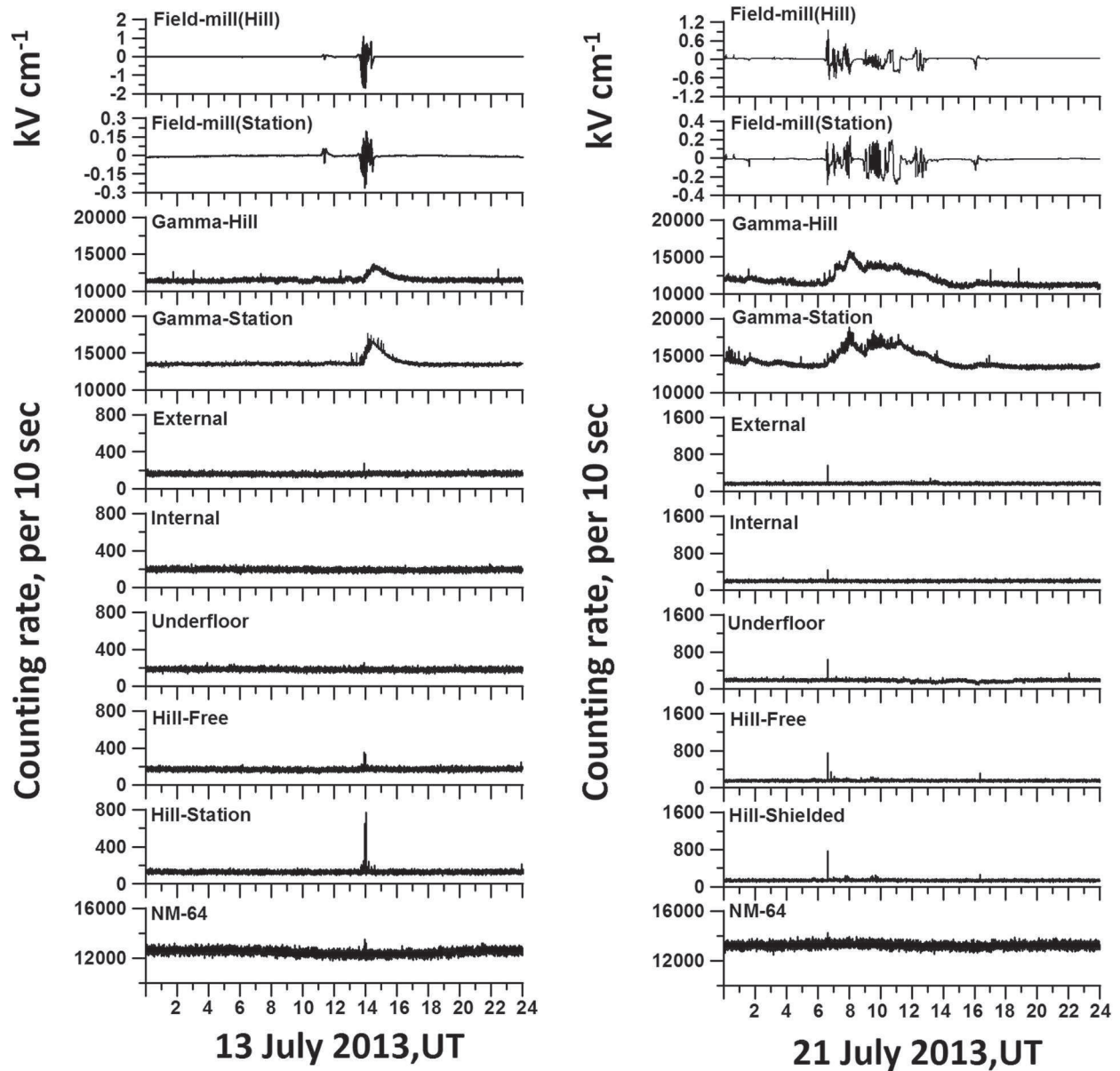


Fig. 3. Monitoring mode results during July 13 and 21, 2013. Detectors are marked in the panels.

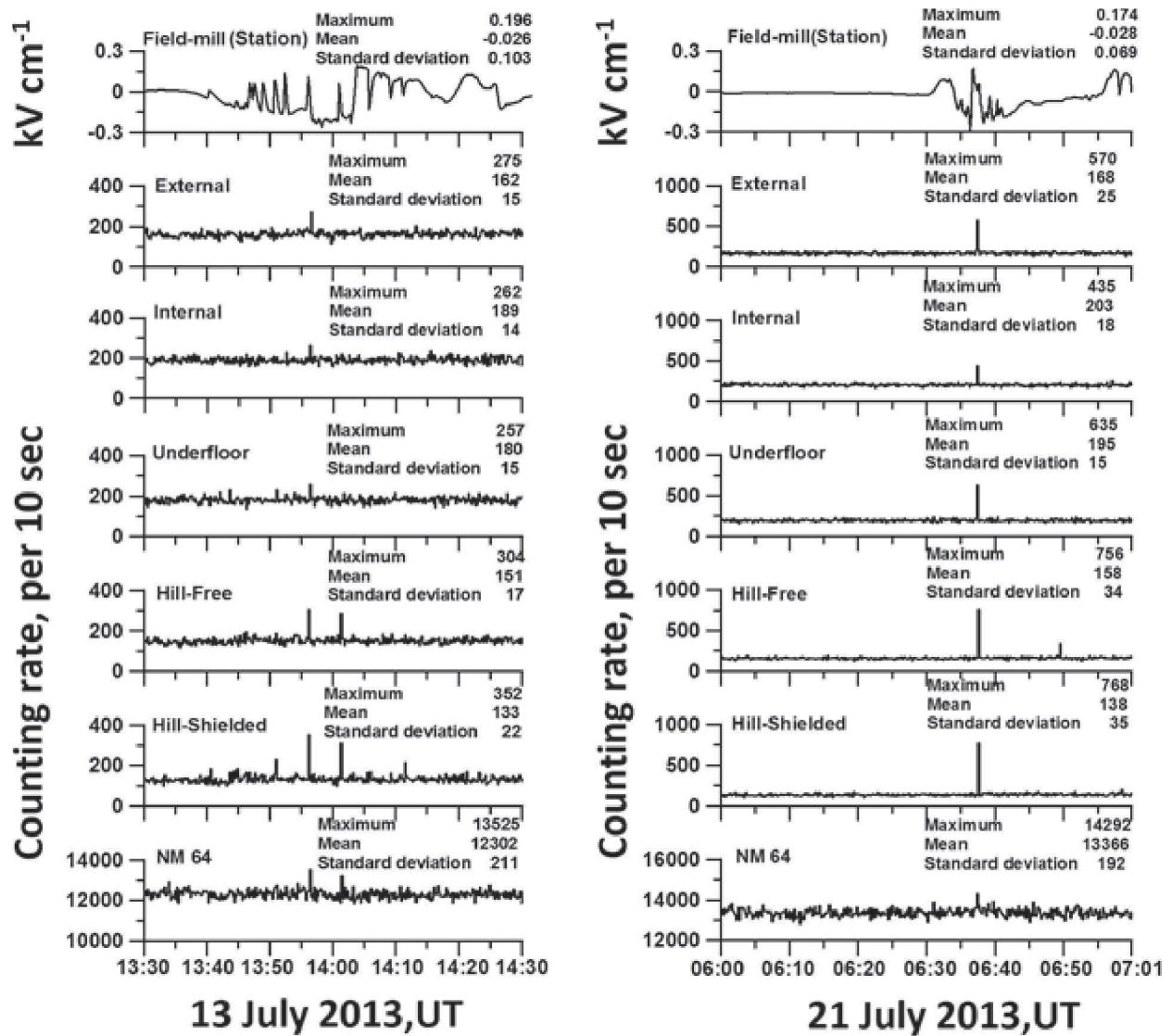


Fig. 4. Monitoring mode results during thunderstorms on July 13 and 21, 2013. Upper panel - electric field as measured by the field-mill detector placed at the Station point, lower panels - count rates in different neutron detectors marked in the panels.

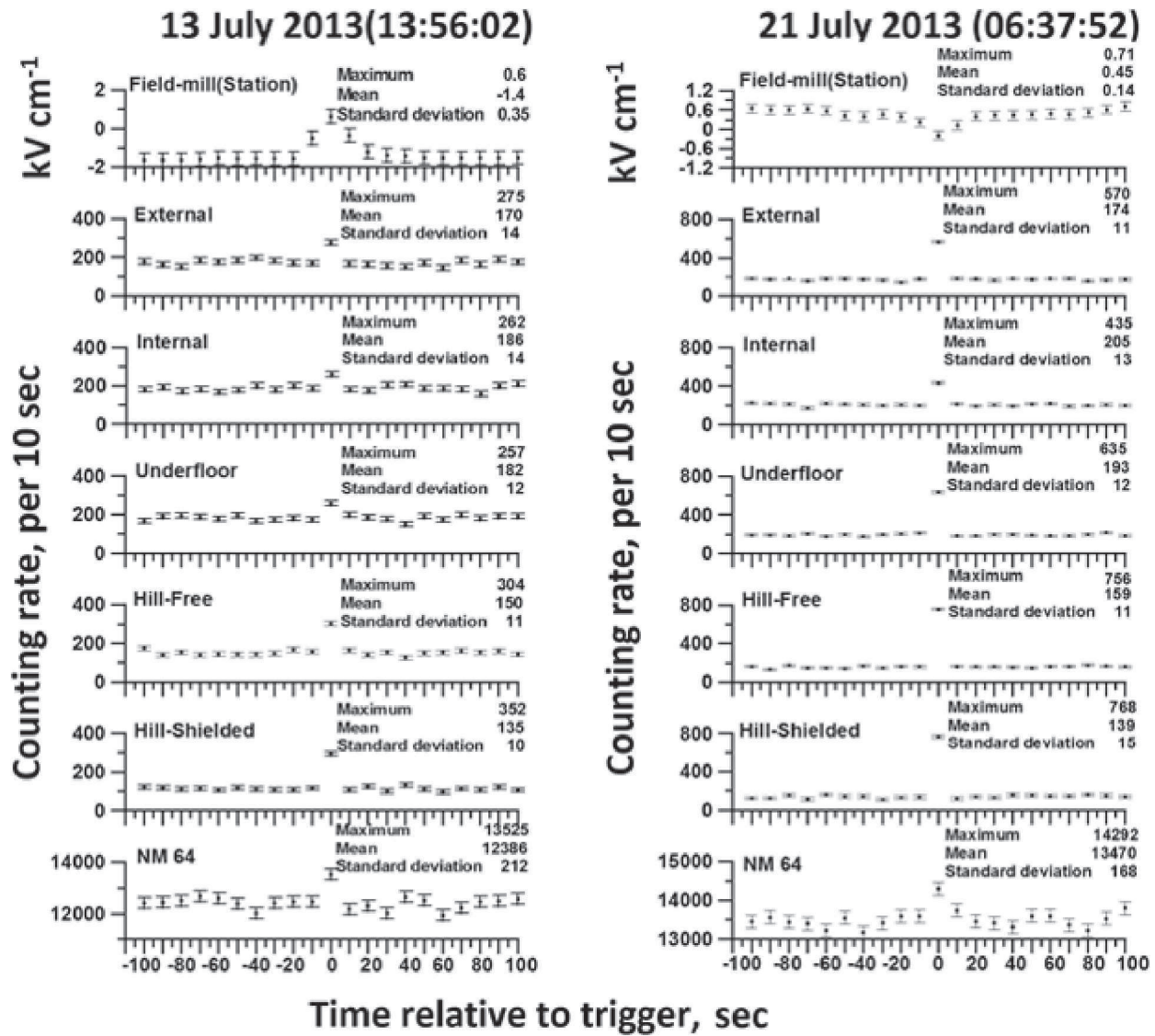


Fig. 5. Examples of neutron count rate enhancements registered in the monitoring mode on July, 13 and 21, 2013, presented with a time scale zoomed in. Panels are the same as in Fig. 4. Zero points marks the middle of a 10-s intervals containing the trigger moments presented in Figs. 6, 7.

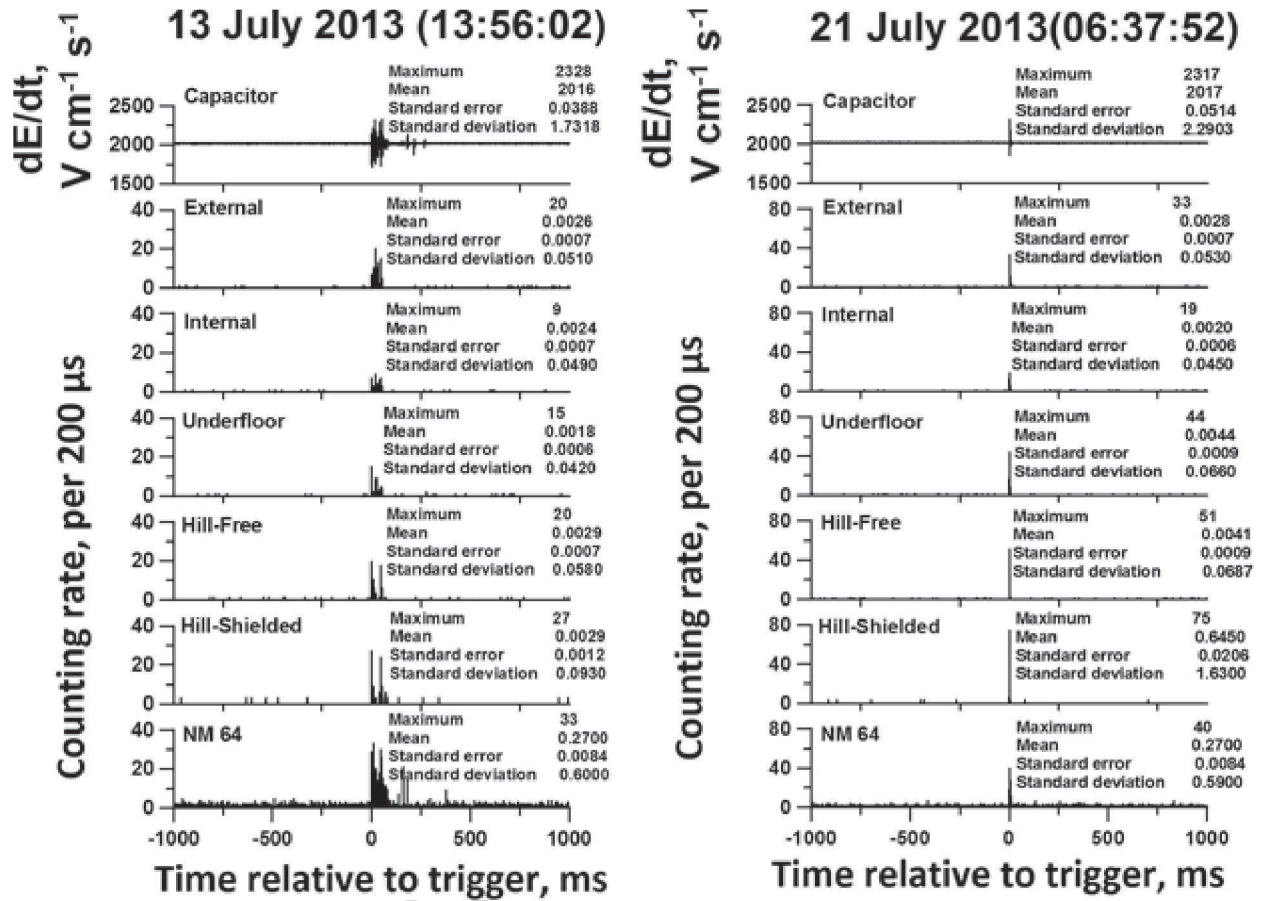


Fig. 6. Time structure of neutron count rate of the discharge 13 July 2013 (13:56:02) and of the discharge 21.07.2013 (06:37:52).

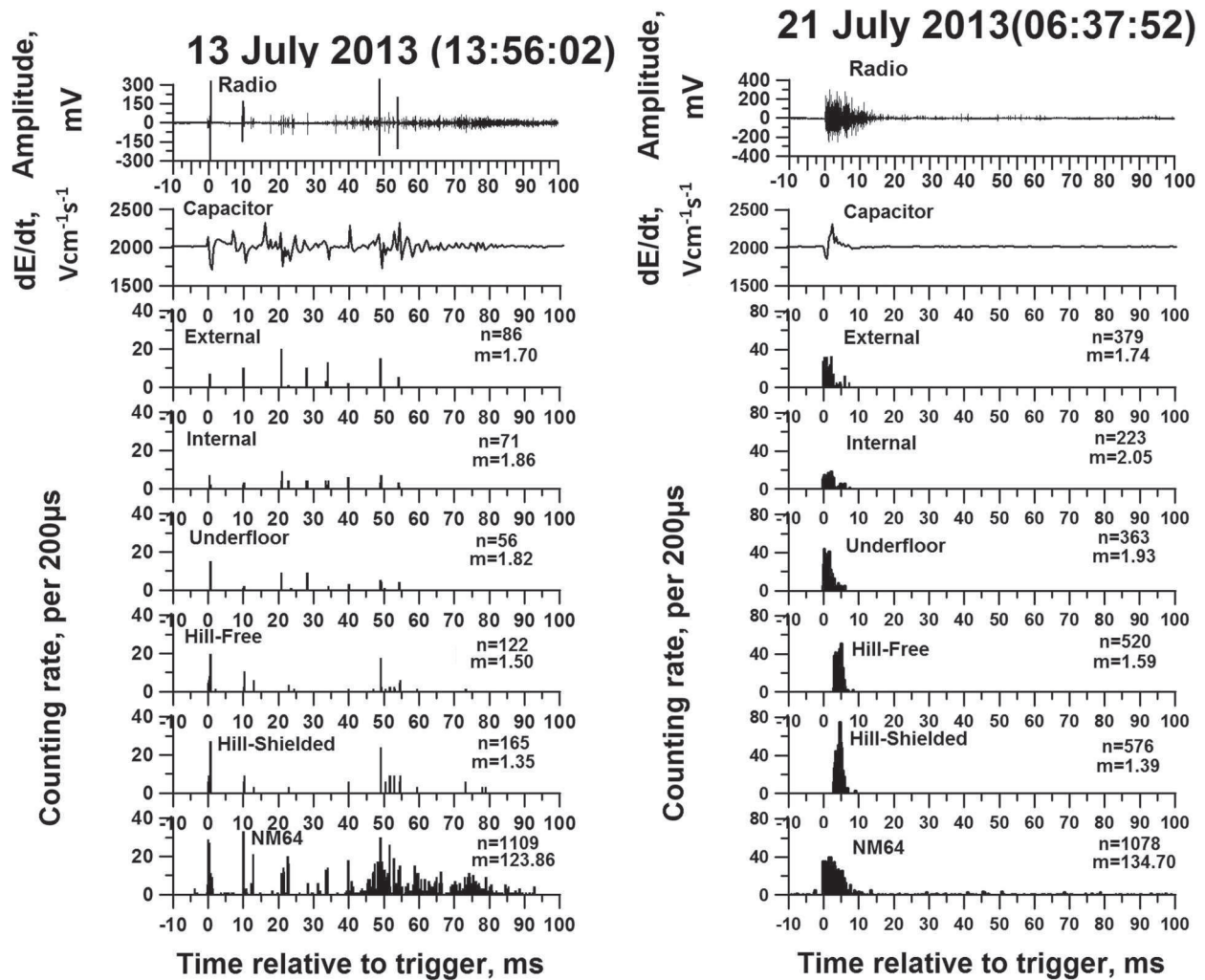


Fig. 7. Fine time structures of neutron count rate of the discharge 13 July 2013 (13:56:02) and of the discharge 21.07.2013 (06:37:52). “n=” – the number of neutrons registered during 100 ms; “m=” – the mean number of neutrons expected for 100 ms from monitoring mode results.

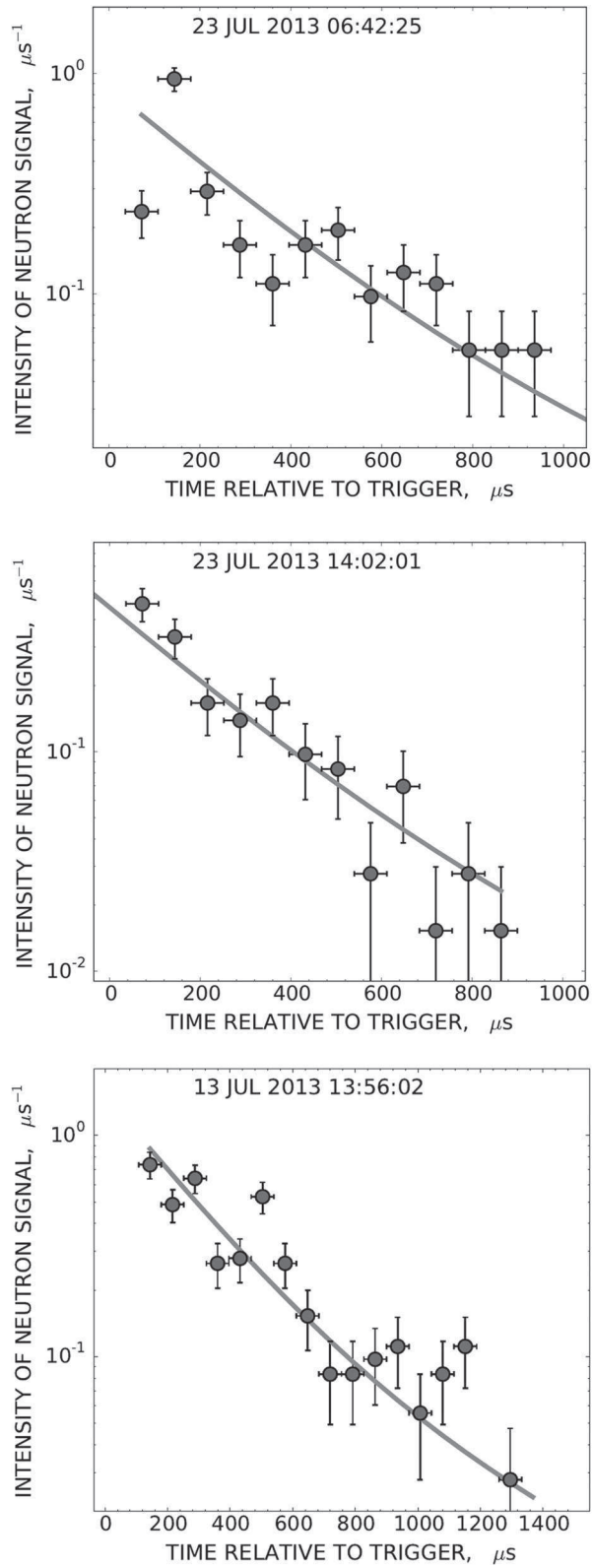


Fig. 8. Examples of the neutron signal time dependencies as registered by the NM fast registration system (circles with error bars). Every plot corresponds to a neutron signal peak registered just at the moment of

trigger arrival. The smooth continuous lines represent the usual exponential distribution anticipated for the neutrons momentary born in the monitor and diffusing inside it later on (see text).

ACCEPTED MANUSCRIPT